

EMBEDDED MINIMAL DISKS: PROPER VERSUS NONPROPER - GLOBAL VERSUS LOCAL

TOBIAS H. COLDING AND WILLIAM P. MINICOZZI II

ABSTRACT. We construct a sequence of (compact) embedded minimal disks in a ball in \mathbf{R}^3 with boundaries in the boundary of the ball and where the curvatures blow up only at the center. The sequence converges to a limit which is not smooth and not proper. If instead the sequence of embedded disks had boundaries in a sequence of balls with radii tending to infinity, then we have shown previously that any limit must be smooth and proper.

0. INTRODUCTION

Consider a sequence of (compact) embedded minimal disks $\Sigma_i \subset B_{R_i} = B_{R_i}(0) \subset \mathbf{R}^3$ with $\partial\Sigma_i \subset \partial B_{R_i}$ and either:

- (a) R_i equal to a finite constant.
- (b) $R_i \rightarrow \infty$.

We will refer to (a) as the *local case* and to (b) as the *global case*. Recall that a surface $\Sigma \subset \mathbf{R}^3$ is said to be properly embedded if it is embedded and the intersection of Σ with any compact subset of \mathbf{R}^3 is compact. We say that a lamination or foliation is proper if each leaf is proper.

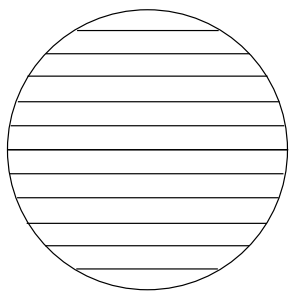


FIGURE 1. The limit in a ball of a sequence of degenerating helicoids is a foliation by parallel planes. This is smooth and proper.

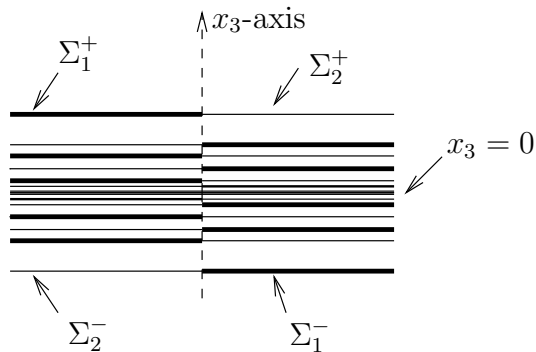


FIGURE 2. A schematic picture of the limit in Theorem 1 which is not smooth and not proper (the dotted x_3 -axis is part of the limit). The limit contains four multi-valued graphs joined at the x_3 -axis; Σ_1^+ , Σ_2^+ above the plane $x_3 = 0$ and Σ_1^- , Σ_2^- below the plane. Each of the four spirals into the plane.

1991 *Mathematics Subject Classification.* 53A10, 49Q05.

The authors were partially supported by NSF Grants DMS 0104453 and DMS 0104187.

We will be interested in the possible limits of sequences of minimal disks Σ_i as above where the curvatures blow up, e.g., $\sup_{B_1 \cap \Sigma_i} |A|^2 \rightarrow \infty$ as $i \rightarrow \infty$. In the global case, Theorem 0.1 in [CM2] gives a subsequence converging off a Lipschitz curve to a foliation by parallel planes; cf. fig. 1. In particular, the limit is a (smooth) foliation which is proper. We show here in Theorem 1 that smoothness and properness of the limit can fail in the local case; cf. fig. 2.

We will need the notion of a multi-valued graph; see fig. 3. Let $D_r \subset \mathbf{C}$ be the disk in the plane centered at the origin and of radius r and let \mathcal{P} be the universal cover of the punctured plane $\mathbf{C} \setminus \{0\}$ with global polar coordinates (ρ, θ) so $\rho > 0$ and $\theta \in \mathbf{R}$. An N -valued graph on the annulus $D_s \setminus D_r$ is a single valued graph of a function u over $\{(\rho, \theta) \mid r < \rho \leq s, |\theta| \leq N\pi\}$.

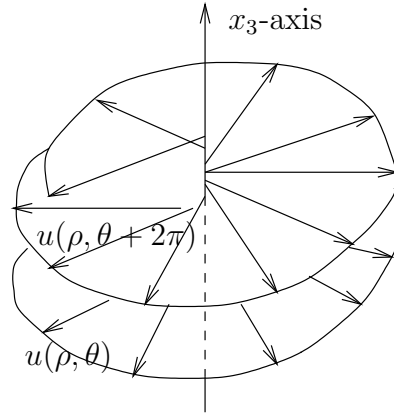


FIGURE 3. A multi-valued graph of a function u .

In Theorem 1, we construct a sequence of disks $\Sigma_i \subset B_1 = B_1(0) \subset \mathbf{R}^3$ as above where the curvatures blow up only at 0 (see (1) and (2)) and $\Sigma_i \setminus \{x_3\text{-axis}\}$ consists of two multi-valued graphs for each i ; see (3). Furthermore (see (4)), $\Sigma_i \setminus \{x_3 = 0\}$ converges to two embedded minimal disks $\Sigma^- \subset \{x_3 < 0\}$ and $\Sigma^+ \subset \{x_3 > 0\}$ each of which spirals into $\{x_3 = 0\}$ and thus is not proper; see fig. 2.

Theorem 1. *There is a sequence of compact embedded minimal disks $0 \in \Sigma_i \subset B_1 \subset \mathbf{R}^3$ with $\partial \Sigma_i \subset \partial B_1$ and containing the vertical segment $\{(0, 0, t) \mid |t| < 1\} \subset \Sigma_i$ so:*

- (1) $\lim_{i \rightarrow \infty} |A_{\Sigma_i}|^2(0) = \infty$.
- (2) $\sup_i \sup_{\Sigma_i \setminus B_\delta} |A_{\Sigma_i}|^2 < \infty$ for all $\delta > 0$.
- (3) $\Sigma_i \setminus \{x_3\text{-axis}\} = \Sigma_{1,i} \cup \Sigma_{2,i}$ for multi-valued graphs $\Sigma_{1,i}$ and $\Sigma_{2,i}$.
- (4) $\Sigma_i \setminus \{x_3 = 0\}$ converges to two embedded minimal disks $\Sigma^\pm \subset \{\pm x_3 > 0\}$ with $\overline{\Sigma^\pm} \setminus \Sigma^\pm = B_1 \cap \{x_3 = 0\}$. Moreover, $\Sigma^\pm \setminus \{x_3\text{-axis}\} = \Sigma_1^\pm \cup \Sigma_2^\pm$ for multi-valued graphs Σ_1^\pm and Σ_2^\pm each of which spirals into $\{x_3 = 0\}$; see fig. 2.

It follows from (4) that $\Sigma_i \setminus \{0\}$ converges to a lamination of $B_1 \setminus \{0\}$ (with leaves Σ^- , Σ^+ , and $B_1 \cap \{x_3 = 0\} \setminus \{0\}$) which does not extend to a lamination of B_1 . Namely, 0 is not a removable singularity.

The multi-valued graphs that we will consider will never close up; in fact they will all be embedded. The most important example of an embedded minimal multi-valued graph

comes from the helicoid. The *helicoid* is the minimal surface Σ in \mathbf{R}^3 parametrized by $(s \cos t, s \sin t, t)$ where $s, t \in \mathbf{R}$. Thus $\Sigma \setminus \{x_3\text{-axis}\} = \Sigma_1 \cup \Sigma_2$, where Σ_1, Σ_2 are ∞ -valued graphs on $\mathbf{C} \setminus \{0\}$. Σ_1 is the graph of the function $u_1(\rho, \theta) = \theta$ and Σ_2 is the graph of the function $u_2(\rho, \theta) = \theta + \pi$.

We will use standard (x_1, x_2, x_3) coordinates on \mathbf{R}^3 and $z = x + iy$ on \mathbf{C} . Given $f : \mathbf{C} \rightarrow \mathbf{C}^n$, $\partial_x f$ and $\partial_y f$ denote $\frac{\partial f}{\partial x}$ and $\frac{\partial f}{\partial y}$, respectively; similarly, $\partial_z f = (\partial_x f - i\partial_y f)/2$. For $p \in \mathbf{R}^3$ and $s > 0$, the ball in \mathbf{R}^3 is $B_s(p)$. K_Σ is the sectional curvature of a smooth surface Σ . When Σ is immersed in \mathbf{R}^3 , then A_Σ will be its second fundamental form (so when Σ is minimal, then $|A_\Sigma|^2 = -2K_\Sigma$). When Σ is oriented, \mathbf{n}_Σ is the unit normal.

1. PRELIMINARIES ON THE WEIERSTRASS REPRESENTATION

Let $\Omega \subset \mathbf{C}$ be a domain. The classical Weierstrass representation (see [Os]) starts from a meromorphic function g on Ω and a holomorphic one-form ϕ on Ω and associates a (branched) conformal minimal immersion $F : \Omega \rightarrow \mathbf{R}^3$ by

$$F(z) = \operatorname{Re} \int_{\zeta \in \gamma_{z_0, z}} \left(\frac{1}{2} (g^{-1}(\zeta) - g(\zeta)), \frac{i}{2} (g^{-1}(\zeta) + g(\zeta)), 1 \right) \phi(\zeta). \quad (1.1)$$

Here $z_0 \in \Omega$ is a fixed base point and the integration is along a path $\gamma_{z_0, z}$ from z_0 to z . The choice of z_0 changes F by adding a constant. We will assume that $F(z)$ does not depend on the choice of path $\gamma_{z_0, z}$; this is the case, for example, when g has no zeros or poles and Ω is simply connected.

The unit normal \mathbf{n} and Gauss curvature K of the resulting surface are then (see sections 8, 9 in [Os])

$$\mathbf{n} = (2 \operatorname{Re} g, 2 \operatorname{Im} g, |g|^2 - 1) / (|g|^2 + 1), \quad (1.2)$$

$$K = - \left[\frac{4 |\partial_z g| |g|}{|\phi| (1 + |g|^2)^2} \right]^2. \quad (1.3)$$

Since the pullback $F^*(dx_3)$ is $\operatorname{Re} \phi$ by (1.1), ϕ is usually called the *height differential*. By (1.2), g is the composition of the Gauss map followed by stereographic projection.

To ensure that F is an immersion (i.e., $dF \neq 0$), we will assume that ϕ does not vanish and g has no zeros or poles. The two standard examples are

$$g(z) = z, \phi(z) = dz/z, \Omega = \mathbf{C} \setminus \{0\} \text{ giving a catenoid,} \quad (1.4)$$

$$g(z) = e^{iz}, \phi(z) = dz, \Omega = \mathbf{C} \text{ giving a helicoid.} \quad (1.5)$$

The next lemma records the differential of F .

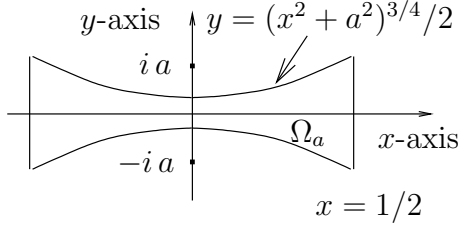
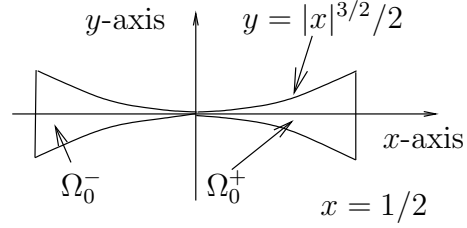
Lemma 1. *If F is given by (1.1) with $g(z) = e^{i(u(z)+iv(z))}$ and $\phi = dz$, then*

$$\partial_x F = (\sinh v \cos u, \sinh v \sin u, 1), \quad (1.6)$$

$$\partial_y F = (\cosh v \sin u, -\cosh v \cos u, 0). \quad (1.7)$$

2. THE PROOF OF THEOREM 1

To show Theorem 1, we first construct a one-parameter family (with parameter $a \in (0, 1/2)$) of minimal immersions F_a by making a specific choice of Weierstrass data $g = e^{ih_a}$ (where $h_a = u_a + i v_a$), $\phi = dz$, and domain Ω_a to use in (1.1). We show in Lemma 2 that this one-parameter family of immersions is compact. Lemma 3 shows that the immersions $F_a : \Omega_a \rightarrow \mathbf{R}^3$ are embeddings.

FIGURE 4. The domain Ω_a .FIGURE 5. $\Omega_0 = \cap_{a>0} \Omega_a \setminus \{0\}$ and its two components Ω_0^+ and Ω_0^- .

For each $0 < a < 1/2$, set (see fig. 4)

$$h_a(z) = \frac{1}{a} \arctan\left(\frac{z}{a}\right) \text{ on } \Omega_a = \{(x, y) \mid |x| \leq 1/2, |y| \leq (x^2 + a^2)^{3/4}/2\}. \quad (2.1)$$

Note that h_a is well-defined since Ω_a is simply connected and $\pm ia \notin \Omega_a$. For future reference

$$\partial_z h_a(z) = \frac{1}{z^2 + a^2} = \frac{x^2 + a^2 - y^2 - 2i xy}{(x^2 + a^2 - y^2)^2 + 4x^2 y^2}, \quad (2.2)$$

$$K_a(z) = \frac{-|\partial_z h_a|^2}{\cosh^4 v_a} = \frac{-|z^2 + a^2|^{-2}}{\cosh^4(\operatorname{Im} \arctan(z/a)/a)}. \quad (2.3)$$

Here (2.3) used (1.3). Note that, by the Cauchy-Riemann equations,

$$\partial_z h_a = (\partial_x - i \partial_y)(u_a + i v_a)/2 = \partial_x u_a - i \partial_y u_a = \partial_y v_a + i \partial_x v_a. \quad (2.4)$$

In the rest of this paper we let $F_a : \Omega_a \rightarrow \mathbf{R}^3$ be from (1.1) with $g = e^{ih_a}$, $\phi = dz$, and $z_0 = 0$. Set $\Omega_0 = \cap_a \Omega_a \setminus \{0\}$, so $\Omega_0 = \{(x, y) \mid 0 < |x| \leq 1/2, |y| \leq |x|^{3/2}/2\}$; see fig. 5. The family of functions h_a is not compact since $\lim_{a \rightarrow 0} |h_a|(z) = \infty$ for $z \in \Omega_0$. However, the next lemma shows that the family of immersions F_a is compact.

Lemma 2. *If $a_j \rightarrow 0$, then there is a subsequence a_i so F_{a_i} converges uniformly in C^2 on compact subsets of Ω_0 .*

Proof. Since h_a and $-1/z$ are holomorphic and

$$|\partial_z h_a(z) - \partial_z(-1/z)| = a^2 |z|^{-2} |z^2 + a^2|^{-1}, \quad (2.5)$$

we get easily that ∇h_a converges as $a \rightarrow 0$ to $\nabla(-1/z)$ uniformly on compact subsets of Ω_0 . Since each $v_a(x, 0) = 0$, the fundamental theorem of calculus gives that the v_a 's converge uniformly in C^1 on compact subsets of Ω_0 . (Unfortunately, the u_a 's do not converge.)

Let $\Omega_0^\pm = \{\pm x > 0\} \cap \Omega_0$ be the two components of Ω_0 ; see fig. 5. Set $b_j^+ = u_{a_j}(1/2)$ and $b_j^- = u_{a_j}(-1/2)$ and choose a subsequence a_i so both b_i^- and b_i^+ converge modulo 2π (this is possible since $T^2 = \mathbf{R}^2/(2\pi\mathbf{Z}^2)$ is compact). Arguing as above, $h_{a_i} - b_i^\pm$ converges

uniformly in C^1 on compact subsets of Ω_0^\pm . Therefore, by Lemma 1, the minimal immersions corresponding to Weierstrass data $g = e^{i(h_{a_i} - b_i^\pm)}$, $\phi = dz$ converge uniformly in C^2 on compact subsets of Ω_0^\pm as $i \rightarrow \infty$. \square

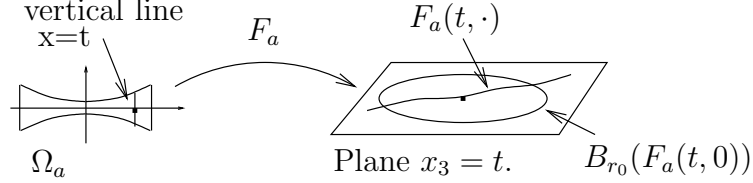


FIGURE 6. A horizontal slice in Lemma 3.

The main difficulty in proving Theorem 1 is showing that the immersions $F_a : \Omega_a \rightarrow \mathbf{R}^3$ are embeddings. This will follow easily from (A) and (B) below. Namely, we show in Lemma 3, see fig. 6 and 7, that for $|t| \leq 1/2$:

- (A) The horizontal slice $\{x_3 = t\} \cap F_a(\Omega_a)$ is the image of the vertical segment $\{x = t\}$ in the plane, i.e., $x_3(F_a(x, y)) = x$; see (2.6).
- (B) The image $F_a(\{x = t\} \cap \Omega_a)$ is a graph over a line segment in the plane $\{x_3 = t\}$ (the line segment will depend on t); see (2.7).
- (C) The boundary of the graph in (B) is outside the ball $B_{r_0}(F_a(t, 0))$ for some $r_0 > 0$ and all a ; see (2.8).

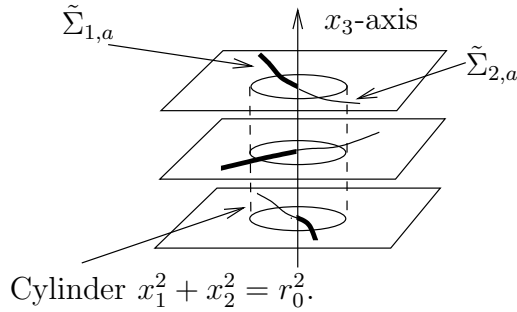


FIGURE 7. Horizontal slices of $F_a(\Omega_a)$ in Lemma 3.

Lemma 3.

$$x_3(F_a(x, y)) = x. \quad (2.6)$$

$$\text{The curve } F_a(x, \cdot) : [-(x^2 + a^2)^{3/4}/2, (x^2 + a^2)^{3/4}/2] \rightarrow \{x_3 = x\} \text{ is a graph.} \quad (2.7)$$

$$|F_a(x, \pm(x^2 + a^2)^{3/4}/2) - F_a(x, 0)| > r_0 \text{ for some } r_0 > 0 \text{ and all } a. \quad (2.8)$$

Proof. Since $z_0 = 0$ and $\phi = dz$, we get (2.6) from (1.1). Using $y^2 < (x^2 + a^2)/4$ on Ω_a , (2.2) and (2.4) give

$$|\partial_y u_a(x, y)| = \frac{2|xy|}{(x^2 + a^2 - y^2)^2 + 4x^2 y^2} \leq \frac{4|xy|}{(x^2 + a^2)^2}, \quad (2.9)$$

$$\partial_y v_a(x, y) = \frac{x^2 + a^2 - y^2}{(x^2 + a^2 - y^2)^2 + 4x^2 y^2} > \frac{3}{8(x^2 + a^2)}. \quad (2.10)$$

Set $y_{x,a} = (x^2 + a^2)^{3/4}/2$. Integrating (2.9) gives

$$\max_{|y| \leq y_{x,a}} |u_a(x, y) - u_a(x, 0)| \leq \int_0^{y_{x,a}} \frac{4|xt|}{(x^2 + a^2)^2} dt = \frac{|x|}{2(x^2 + a^2)^{1/2}} < 1. \quad (2.11)$$

Set $\gamma_{x,a}(y) = F_a(x, y)$. Since $v_a(x, 0) = 0$ and $\cos(1) > 1/2$, combining (1.7) and (2.11) gives

$$\langle \gamma'_{x,a}(y), \gamma'_{x,a}(0) \rangle = \cosh v_a(x, y) \cos(u_a(x, y) - u_a(x, 0)) > \cosh v_a(x, y)/2. \quad (2.12)$$

Here $\gamma'_{x,a}(y) = \partial_y F_a(x, y)$. By (2.12), the angle between $\gamma'_{x,a}(y)$ and $\gamma'_{x,a}(0)$ is always less than $\pi/2$; this gives (2.7). Since $v_a(x, 0) = 0$, integrating (2.10) gives

$$\min_{y_{x,a}/2 \leq |y| \leq y_{x,a}} |v_a(x, y)| \geq \int_0^{y_{x,a}} \frac{3 dt}{8(x^2 + a^2)} = \frac{3}{32(x^2 + a^2)^{1/4}}. \quad (2.13)$$

Integrating (2.12) and using (2.13) gives

$$\langle \gamma_{x,a}(y_{x,a}) - \gamma_{x,a}(0), \gamma'_{x,a}(0) \rangle > \frac{(x^2 + a^2)^{3/4}}{16} e^{(x^2 + a^2)^{-1/4}/11}. \quad (2.14)$$

Since $\lim_{s \rightarrow 0} s^3 e^{s^{-1}/11} = \infty$, (2.14) and its analog for $\gamma_{x,a}(-y_{x,a})$ give (2.8). \square

Corollary 1. *See fig. 7. Let r_0 be given by (2.8).*

- (i) F_a is an embedding.
- (ii) $F_a(t, 0) = (0, 0, t)$ for $|t| < 1/2$.
- (iii) $\{0 < x_1^2 + x_2^2 < r_0^2\} \cap F_a(\Omega_a) = \tilde{\Sigma}_{1,a} \cup \tilde{\Sigma}_{2,a}$ for multi-valued graphs $\tilde{\Sigma}_{1,a}, \tilde{\Sigma}_{2,a}$ over $D_{r_0} \setminus \{0\}$.

Proof. Equations (2.6) and (2.7) immediately give (i).

Since $z_0 = 0$, $F(0, 0) = (0, 0, 0)$. Integrating (1.6) and using $v_a(x, 0) = 0$ then gives (ii).

By (1.2), F_a is “vertical,” i.e., $\langle \mathbf{n}, (0, 0, 1) \rangle = 0$, when $|g_a| = 1$. However, $|g_a(x, y)| = 1$ exactly when $y = 0$ so that, by (ii), the image is graphical away from the x_3 -axis. Combining this with (2.8) gives (iii). \square

Corollary 1 constructs the embeddings F_a that will be used in Theorem 1 and shows property (3). To prove Theorem 1, we need therefore only show (1), (2), and (4).

Proof. (of Theorem 1). By scaling, it suffices to find a sequence $\Sigma_i \subset B_R$ for some $R > 0$. Corollary 1 gives minimal embeddings $F_a : \Omega_a \rightarrow \mathbf{R}^3$ with $F_a(t, 0) = (0, 0, t)$ for $|t| < 1/2$ and so (3) holds for any $R \leq r_0$. Set $R = \min\{r_0/2, 1/4\}$ and $\Sigma_i = B_R \cap F_{a_i}(\Omega_{a_i})$, where the sequence a_i is to be determined.

To get (1), simply note that, by (2.3), $|K_a|(0) = a^{-4} \rightarrow \infty$ as $a \rightarrow 0$.

We next show (2). First, by (2.3), $\sup_a \sup_{\{|x| \geq \delta\} \cap \Omega_a} |K_a| < \infty$ for all $\delta > 0$. Combined with (3) and Heinz’s curvature estimate for minimal graphs (i.e., 11.7 in [Os]), this gives (2).

To get (4), use Lemma 2 to choose $a_i \rightarrow 0$ so the mappings F_{a_i} converge uniformly in C^2 on compact subsets to $F_0 : \Omega_0 \rightarrow \mathbf{R}^3$. Hence, by Lemma 3, $\Sigma_i \setminus \{x_3 = 0\}$ converges to two embedded minimal disks $\Sigma^\pm \subset F_0(\Omega_0^\pm)$ with $\Sigma^\pm \setminus \{x_3\text{-axis}\} = \Sigma_1^\pm \cup \Sigma_2^\pm$ for multi-valued graphs Σ_j^\pm . To complete the proof, we show that each graph Σ_j^\pm is ∞ -valued (and, hence, spirals into $\{x_3 = 0\}$). Note that, by (3) and (1.7), the level sets $\{x_3 = x\} \cap \Sigma_j^\pm$ are graphs over the line in the direction

$$\lim_{a \rightarrow 0} (\sin u_a(x, 0), -\cos u_a(x, 0), 0). \quad (2.15)$$

Therefore, since an easy calculation gives for $0 < t < 1/4$ that

$$\lim_{a \rightarrow 0} |u_a(t, 0) - u_a(2t, 0)| = 1/(2t), \quad (2.16)$$

we see that $\{t < |x_3| < 2t\} \cap \Sigma_j^\pm$ contains an embedded N_t -valued graph where $N_t \approx 1/(4\pi t) \rightarrow \infty$ as $t \rightarrow 0$. It follows that Σ_j^\pm must spiral into $\{x_3 = 0\}$, completing (4). \square

REFERENCES

- [CM1] T.H. Colding and W.P. Minicozzi II, Embedded minimal disks, To appear in The Proceedings of the Clay Mathematics Institute Summer School on the Global Theory of Minimal Surfaces. MSRI. math.DG/0206146.
- [CM2] ———, The space of embedded minimal surfaces of fixed genus in a 3-manifold IV; Locally simply connected, preprint, math.AP/0210119.
- [Os] R. Osserman, A survey of minimal surfaces, *Dover*, 2nd. edition (1986).

COURANT INSTITUTE OF MATHEMATICAL SCIENCES AND PRINCETON UNIVERSITY, 251 MERCER STREET,
NEW YORK, NY 10012 AND FINE HALL, WASHINGTON RD., PRINCETON, NJ 08544-1000

DEPARTMENT OF MATHEMATICS, JOHNS HOPKINS UNIVERSITY, 3400 N. CHARLES ST., BALTIMORE,
MD 21218

E-mail address: colding@cims.nyu.edu, minicozz@jhu.edu